

by the (p, n) time-of-flight measurements for the energy region 944 to 3080 keV, the present data have yielded branching ratios which should prove to be of great utility in the theoretical attempts to describe the states of ^{93}Mo . A new area of interest has also been provided with the new states above 3.7 MeV which had been previously unrecorded by the noncoincidence pickup and stripping experiments.

*Work supported in part by the Robert A. Welch Foundation and the U. S. Atomic Energy Commission.

† Present address: Teledyne Isotopes, Westwood, New Jersey.

¹K. H. Bhatt and J. B. Ball, Nucl. Phys. **63**, 286 (1965).

²K. P. Lieb, T. Hausmann, and J. J. Kent, Phys. Rev. **182**, 1341 (1969).

³D. C. Choudhury and J. T. Clemens, Nucl. Phys. **A125**, 140 (1969).

⁴P. Alexander and G. Scharff-Goldhaber, Phys. Rev. **151**, 964 (1966).

⁵S. A. Hjorth and B. L. Cohen, Phys. Rev. **135**, B920 (1964).

⁶J. B. Moorhead and R. A. Moyer, Phys. Rev. **184**, 1205 (1969).

⁷R. C. Diehl, B. L. Cohen, R. A. Moyer, and L. H. Goldman, Phys. Rev. C **1**, 2132 (1970).

⁸H. J. Kim, R. L. Robinson, C. H. Johnson, and S. Raman, Nucl. Phys. **A142**, 35 (1970).

⁹C. Maples, G. W. Goth, and J. Cerny, University of California Radiation Laboratory Report No. UCRL-16964, 1966 (unpublished).

¹⁰J. B. Ball, private communication.

Hyperfine Structure and Isomeric Shift of $\text{Hg}^{199m\ddagger}$

Robert L. Covey* and Sumner P. Davis

Physics Department, University of California, Berkeley, California 94720

(Received 2 December 1971)

The optical hyperfine structure and isotope shift in the 2537-Å line have been investigated. Two of the three components have been observed and measured. The magnetic-dipole-splitting factor $A(^3P_1)$ is $-0.0771 \pm 0.0005 \text{ cm}^{-1}$ and the isotope shift $\Delta S(^1S_0)$ is $0.112 \pm 0.006 \text{ cm}^{-1}$ with respect to Hg^{198} . The shift indicates staggering toward the heavier even isotope. An explanation is given in terms of nuclear deformation.

INTRODUCTION

High-resolution optical spectroscopy is a means of studying the electromagnetic properties of many heavy nuclei. In recent years the hyperfine structure and isotopic shift of artificially produced radioisotopes have been observed and measured.¹⁻³ We report in this paper the measurement of the magnetic-hyperfine-splitting factor and isotope shift of the Hg^{199m} isomer of the optical transition $^3P_1-^1S_0$ at 2537 Å. This isomer has a half-life of 44 min, and a nuclear spin⁴ of $\frac{13}{2}$. The upper 3P_1 level is split into three by magnetic hyperfine interaction, while the ground 1S_0 level is shifted by nuclear volume isotope effects.

LIGHT SOURCE PRODUCTION AND OBSERVATION

A platinum target is required for production of mercury isotopes with $N > 118$ by simple charged-particle bombardment in quantities sufficient for spectroscopic observation. Our choices of reactions were initially both $\text{Pt}^{196}(\alpha, n)\text{Hg}^{199m}$ and $\text{Pt}^{198}(\alpha, 3n)\text{Hg}^{199m}$, but we found that the latter reaction had a much larger cross section at its peaking energy. In addition, its higher α -particle energy

was more favorable to the production of the metastable rather than the ground state of Hg^{199} . Several hundred milligrams of platinum enriched to 34.9% in the 198 isotope (leaving 33.5% in the 196 isotope) were purchased from the Oak Ridge National Laboratory and used to make the target foil. The 88-in. cyclotron at the Lawrence Radiation Laboratory in Berkeley was used for the bombardments. It could provide α -particle energies up to 120 MeV at external beam currents of 40 μA .

Trial bombardments of the enriched foil were made to determine the optimum energy for production of Hg^{199m} . The isomer was detected by observation of 158- and 373-keV γ rays resulting from the decay to the ground state. The peak cross section was $280 \pm 60 \text{ mb}$ at an energy of $34.5 \pm 1 \text{ MeV}$. The energy was raised to 38 MeV in bombardment of the actual foils used for preparation of the light sources to allow for a degradation of 7 MeV in passing through a foil of thickness 2 mil. The maximum amount of isomer produced was 3×10^{13} atoms, limited by the 35% sample enrichment, 2-mil target foil thickness, and 40- μA beam current. Bombardment times were

30 to 45 min.

Preparation of the target foil was a critical procedure because it had to be free of both hydrocarbon and natural mercury contamination. Organic impurities and water vapor seriously reduced the mercury excitation, while natural mercury masked any radioisotopes produced. The spongy platinum granules obtained from Oak Ridge were first melted in a MgO crucible in an electric furnace, and then remelted with a torch onto a siliceous refractory brick. The single bead was etched in hot 50% concentrated hydrofluoric acid for several minutes, after which it was pressed to a thickness of 20 mil between stainless-steel blocks in a hydraulic press. The foil was then rolled with frequent annealing to a final thickness of 2 mil. It was again etched, heated, outgassed in a vacuum furnace for 24 h, and sealed in an evacuated quartz capsule until placed in the cyclotron target holder.

Fabrication of the discharge tube was somewhat different from earlier work.² Blank tubes were made with a plasma melting section 25 mm in diameter and a discharge section 7 mm in diameter. The radioactive target foil was rolled into a small cylinder, sealed into the large section

of the blank, and the blank attached to the vacuum system. It was cleaned, outgassed, and filled with argon as described earlier.² Then the tube was cut off from the system, the foil melted in an induction heater, the mercury condensed in the discharge section with liquid nitrogen, and the two sections cut apart. The final tube contained about 75% of the radioactive mercury and argon at 2 Torr pressure. On good runs the tube was ready to operate 30 min after beam-off time. The discharge tube was excited with microwave radiation at a frequency of 2450 MHz. External heating with a torch was required to keep the mercury in the discharge. The presence of the green line at 5461 Å as observed in a spectroscope was used as an indication of proper excitation conditions.

Spectrographic observations were made with a plane grating in a 3-m Czerny-Turner mounting. The resolving power was 5×10^5 , the plate factor $3.3 \text{ cm}^{-1}/\text{mm}$. Exposures ranged from 15 sec to 5 min on Kodak spectroscopic plates type 103a-0.

DATA TAKING AND MEASUREMENTS

Spectrum lines from Hg^{199m} were detected on seven separate exposures with sources made from four cyclotron runs. Two of the three predicted components could be observed, but the third was always masked by lines from stable isotopes. Typical spectrograms are shown in Fig. 1, and microdensitometer traces in Figs. 2 and 3. These show the presence of the isomer and its subsequent decay, although the two components of Hg^{199} dominate the exposures. For Hg^{199m} , the $F = \frac{1}{2}$ component is partially blended with the $F = \frac{3}{2}$ com-

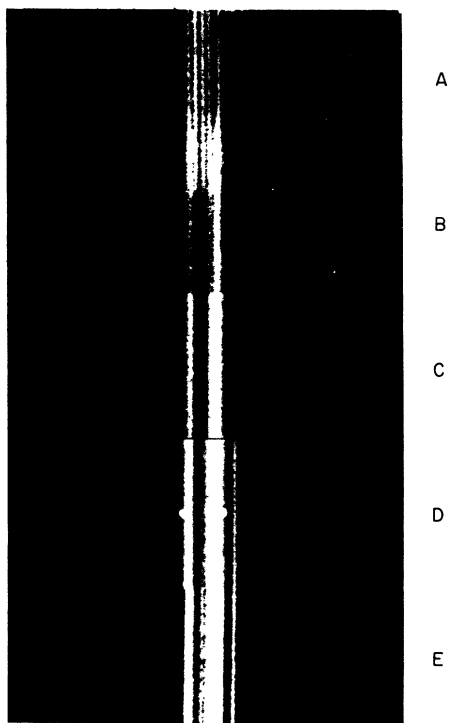


FIG. 1. Spectrograms of the mercury 2537-Å line: A, natural mercury; B, C, D, radioactive mercury about 35 min after beam-off time. The two white dots in D show 199m components; E shows radioactive mercury about 8 h after beam-off time.

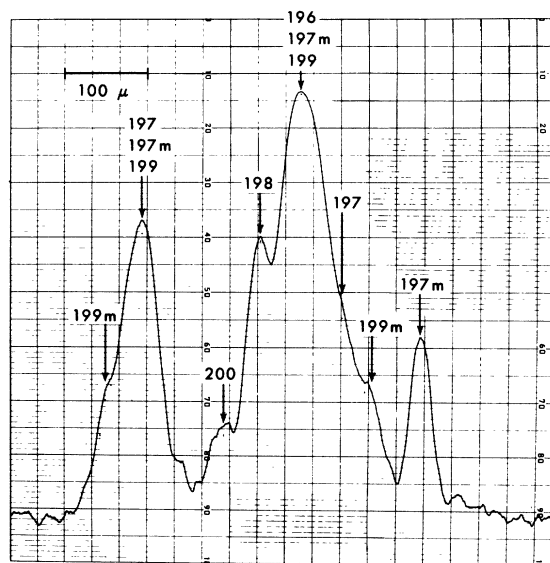


FIG. 2. Microdensitometer trace of the mercury 2537-Å line 35 min after beam-off time.

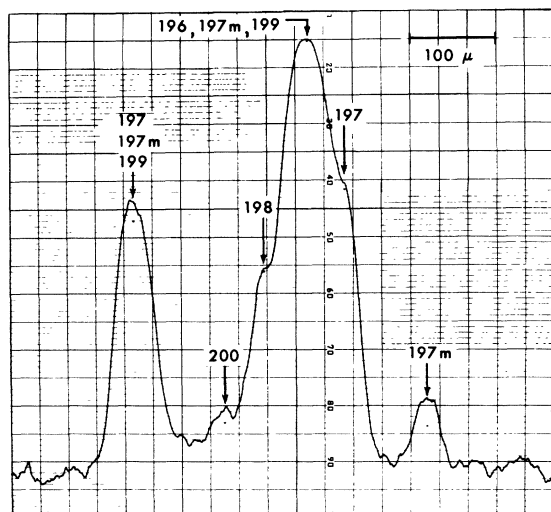


FIG. 3. Microdensitometer trace of the mercury 2537-Å line 21 h after beam-off time.

ponent of 199, and the $F = \frac{15}{2}$ component is blended with the $F = \frac{7}{2}$ component of 199. Measurements of the positions of all components were made with reference to the lines of natural mercury. Each component was measured several times on each spectrogram and a least-squares interpolation made to determine wavelength and wave-number differences. The standard deviations for a single exposure were 0.01 cm^{-1} or less. Systematic errors between exposures, as measured by external consistency, were slightly larger. Statistical errors result mostly from emulsion grain of the photographic plate. Systematic errors are difficult to estimate, because the measurements of partially resolved lines are dependent on subjective conditioning of the observer (even when measuring from traces of the profiles, which we have also done), and on the densities of the exposures. We made trial modifications of the measurements by correcting for blending, but found that it made too little difference to warrant any

systematic changes. The results of averaging all measurements are given in Table I.

INTERPRETATION OF RESULTS AND CONCLUSIONS

There are three independent parameters to be determined: the magnetic-splitting factor $A(^3P_1)$, the quadrupole-splitting factor $B(^3P_1)$, and the isotope shift $\Delta S(^1S_0)$; but we have measured only two components of the spectrum line. The simplest approach is to assume that B has the same value as for the isomer 197m, and to calculate directly the magnetic-splitting factor and isotope shift. We assume a value of -0.026 cm^{-1} , use the data of Table I, and calculate $A(^3P_1) = 0.0771 \pm 0.0005 \text{ cm}^{-1}$ and $\Delta S(^1S_0) = 0.112 \pm 0.006 \text{ cm}^{-1}$ with respect to 198. This method is reasonably accurate because the effect of quadrupole splitting on the component positions is much smaller than the effects of either the isotope shift or the magnetic splitting, and the B factors are very nearly equal for all isomers previously measured.

The magnetic splitting factor is almost the same as for other mercury isomers, which fact is explained by the relative isolation of the odd $I = \frac{15}{2}$ neutron from the nuclear core, and its consequent insensitivity to changes in the core. We calculate the value $\mu_I = (-1.014 \pm 0.006)\mu_N$ from the known relation $IA/(\mu_I/\mu_N) = 0.494 \text{ cm}^{-1}$ for mercury,⁵ neglecting the small effect of the hyperfine anomaly. This value shows a continuation of the gradual decrease in the magnetic moments of the stable isomers with the addition of neutrons.

The value obtained for the isotope shift shows that Hg^{199m} is staggered towards the *heavier* even isotope, the reverse of the generally found case, although the staggering continues the trend for the isomers. Figure 4 illustrates these facts. Because of this result, we should examine our assumptions about the quadrupole splitting. The shifts between isomers are 0.155, 0.158, and 0.187 cm^{-1} in order of increasing neutron number. The isotope shift can be interpreted as the sum

TABLE I. Measurements of the hyperfine-structure components in the 2537-Å line. (All wave numbers are given with respect to the Hg^{198} line in natural Hg.)

Radio mercury isotope assignments	Wave number (cm^{-1})	Previous best values Refs. 1 and 2
197m	646 ± 2	643
199m	456 ± 4	
197	350 ± 4	347
196, 197m, 199	185 ± 3	137, 168, 224
198	2 ± 2	0
200	-156 ± 2	-160
197, 197m, 199	-475 ± 4	-421, -433, -513
199m	-619 ± 6	

of a *uniform* volume effect, and a nuclear-deformation effect. From the results there is clearly a different deformation *change* between 197*m* and 199*m* than between 195*m* and 197*m*. Let us consider how the splitting factor B used above might be affected by these considerations.

We can relate both B and ΔS to a single parameter β by the use of a simplified model for nuclear deformations. Once this is done, β and A can be found by solving the equations relating the displacements of the $F = \frac{1}{2}$ and $\frac{15}{2}$ components. To do this, we consider only collective nuclear deformations into ellipsoids with a single axis of symmetry. The deformations can be either permanent or vibrational, or a combination. For permanent deformations with eccentricity ϵ , the parameter is defined as $\beta = \frac{2}{5}\epsilon$, and the intrinsic quadrupole moment is $Q_0 = \frac{6}{5}eZR^2\beta$, where R is the undeformed nuclear radius. For vibrational deformations, we have corresponding relations for the rms values $\langle Q_0^2 \rangle^{1/2}$ and $\langle \beta^2 \rangle^{1/2}$.

The isotope-shift relation can be written as^{6,7}

$$\frac{\Delta S}{\Delta N} \simeq \frac{d(\Delta E)}{dN} = 8 \frac{5 - 2(1 + \rho)K(Z)}{5 - 2(1 - \rho)K(Z)} \frac{(2ZR/a)^{2(\rho-1)}}{\Gamma^2(2\rho)} \\ \times \pi a^3 \psi^2(0) \frac{Ze^2 R}{2a} \frac{1}{a} \frac{dR}{dN} \left(1 + \frac{3}{2}A \frac{d\beta^2}{dN} \right),$$

where $K(Z) = 1 + 0.106(\alpha Z)^2 + 0.0105(\alpha Z)^4 + \dots$, $\rho = (1 - \alpha^2 Z^2)^{1/2}$, and $R^2 = \frac{5}{3}\langle r^2 \rangle$ is called the equivalent radius. The latter can be found if the proton charge distribution is known. This equation gives the isotope shift directly in terms of deformation differences, provided we can find an experimental value for the constant designated as S_0 in the simplified form $\Delta S = S_0[\Delta N + \kappa \Delta(\beta^2)]$. We can do this by using the measured intrinsic quadrupole moments of Hg^{198, 200, 202} to find the deformations and their differences. We follow closely the work of Meligy.⁸ When we combine these data with those on the isotope shift, we find two values of (S_0/hc) which agree within 5% and which average to $-0.101 \text{ cm}^{-1}/\text{neutron}$ for the 2537-Å line. Shifts

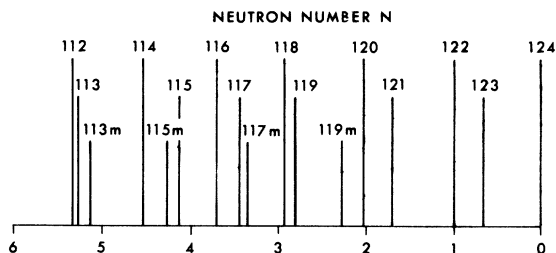


FIG. 4. Relative isotope shifts in the 2537-Å line vs neutron number N . The spacing 122–124 has been normalized to 1.

less than this indicate a deformation decrease, while shifts greater than this indicate an increase. Note that the intrinsic moments given by Meligy include the effects of both permanent and vibrational deformations.

The least certain assumption is that the spectroscopic moment Q is related to the intrinsic moment Q_0 by $Q = Q_0/\gamma$, where γ is a constant dependent only upon the nuclear spin I . In the limit of strong nuclear deformations, the relation is certainly valid, but it may be only qualitatively true for the mercury isotopes. The proximity of the magic number $N = 126$ does not allow strong coupling of the outer nucleons to the core, even though the moderately large intrinsic moments of isotopes 198, 200, and 202 demonstrate collective nuclear behavior (the filled $2d_{3/2}$ subshell has a net vanishing moment in a pure shell model). Furthermore, the spectroscopic moment Q is related only to the *permanent* deformation, which fact further enlarges the effective value of the coupling constant γ . Nevertheless, the computed deformations and B factors of the isomers give $\gamma(193m)/\gamma(195m) = 1.2$ and $\gamma(195m)/\gamma(197m) = 1.1$, so we use $\gamma(197m)/\gamma(199m) = 1.0$.

We have now related the quadrupole factor and the isotope shift to β ; we rewrite the component relations with respect to Hg^{197*m*}, approximate $\Delta(\beta^2)$ by $2\beta\Delta\beta$, and calculate $\Delta\beta$ between 197*m* and 199*m*. We use $\beta(197m) = 0.0734$, $S_0 = -0.101 \text{ cm}^{-1}$, and find $\Delta\beta = -0.0034$ and $\beta(199m) = 0.0700$. Finally, we apply these results to the data for 199*m*, and recalculate the splitting factor A and the isotope shift ΔS . We find that the corrections are entirely negligible.

To summarize, the deformation change between 197*m* and 199*m* is unusually small, and corrections by a more accurate calculation are negligible. Even a large fractional change γ for 199*m* would not change the isotope shift by 1%. A systematic error in the isotope shift comparable to

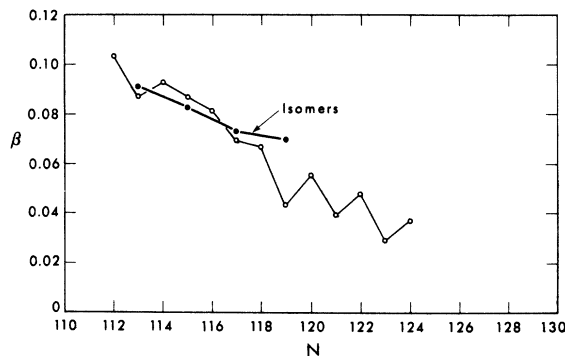


FIG. 5. Deformations β of mercury nuclei as a function of neutron number N .

measurement errors could not be produced by lack of precise knowledge of the position of the third hyperfine-structure component, from which we could calculate a value of B directly.

The deformation calculations have been extended by the same method to all the mercury isotopes for which the isotope-shift data are known, and the results plotted in Fig. 5. The assumed deformation of Hg^{198} has been used together with the average value of the constant S_0 . The odd-even staggering is very pronounced in this plot. The Hg^{199m} isomer shows the only reverse deformation staggering. Because of the proximity of the closed neutron shell at $N=126$, only the lightest mercury isotopes display any significant permanent deformation. Presumably the effective deformation of the heavier isotopes is the result of vibrations about a nearly spherical equilibrium shape. Purely vibrational distortions present no problems in the determination of nuclear deformations from isotope-shift and intrinsic-moment data, since only the rms quantities $\langle Q_0^2 \rangle^{1/2}$ and $\langle \beta^2 \rangle^{1/2}$ are involved. Of course, no meaning can be attached to the deformation sign in such cases. However, the relatively small deformations and consequent weak coupling in most mercury nuclei preclude making an accurate connection between the intrinsic and spectroscopic quadrupole moments. Such considerations show that the calculated nuclear deformations are only semiquantitative. A particular example is the metastable-state spectroscopic moments, which increase slightly with neutron number, while the intrinsic moments $Q_0 = \frac{6}{5} e Z R^2 \beta$ show a more rapid decrease.

We can compute the theoretical uniform volume shift and compare it with the isotope-shift constant S_0 obtained from the nuclear deformations. The best present estimate of the mercury effective electronic wave function at the nucleus for the 2537-Å line is $\psi^2 = 0.98 \times 10^{26} \text{ cm}^{-3}$. We made this estimate by taking account of the contribution of a single 6s electron,⁹ mutual screening of the 6s electrons and screening by the 6p electron,¹⁰ and the direct contribution of the 6p electron.¹¹ The result compares favorably with earlier

ones.^{12, 13} A model for spherical nuclei is the trapezoidal one, with a half-density radius $b = 6.14 F$ and a skin thickness $c = 3.06 F$ for mercury as determined from electron scattering experiments.¹⁴ The isotope-shift formula $d(\Delta E)/dR$ for such nuclei has been discussed by Bodmer⁶ in terms of the equivalent radius $R^2 = \frac{5}{3} \langle r^2 \rangle$, $R = 6.55 F$ for mercury. The additional needed information dR/dN is obtained from $b = b_0 A^{1/3}$ with $b_0 = 1.05 F$. Finally, we obtain $d(\Delta S)/dN = -(1/\hbar c)[d(\Delta E)/dN] = -0.108 \text{ cm}^{-1}/\text{neutron}$ for the mercury 2537-Å line in agreement with $S_0 = -0.101 \text{ cm}^{-1}/\text{neutron}$. It therefore does not seem that additional effects such as nuclear compressibility are necessary to explain the magnitude of the isotope shifts in mercury.

Nevertheless, calculations by Barrett¹⁵ show that the monopole vibrations of the nuclear core induced by an odd neutron in the mercury isotopes can aid in the understanding of both the odd-even staggering and the isomeric shift between the ground and metastable states. Such monopole vibrations are essentially a pulsation in size of a spherical nucleus, and depend on the existence of a finite compressibility of nuclear matter. This type of core excitation can reproduce the change in sign of the isomeric shift in mercury at $N=115$ if the proper kind of internucleon force is postulated. Our results for Hg^{199m} agree only qualitatively with the theory. We can use the volume-shift formula to derive isomeric equivalent proton radius changes of $+0.00215$, -0.00197 , $+0.00143$, and $+0.00806 F$ for $N=113$, 115 , 117 , and 119 , respectively, (compare with $dR/dN = +0.00962 F/\text{neutron}$). The large positive change for Hg^{199m} is not entirely anticipated in the calculations of Barrett which result in $+0.00443 F$ for this isomer, although the direction of the isomeric shift is correctly predicted.

ACKNOWLEDGMENTS

We are grateful for the assistance of C. M. Lederer, R. M. Larimer, J. C. Ehrhardt, D. E. Grimes, and the staff of Environmental Health and Safety.

† Work supported in part by a grant from the National Science Foundation.

*Present address: Institute for Molecular Physics, University of Maryland, College Park, Maryland 20742.

¹S. P. Davis, T. Aung, and H. Kleiman, *Phys. Rev.* **147**, 861 (1966).

²D. Goorvitch, S. P. Davis, and H. Kleiman, *Phys. Rev.* **188**, 1897 (1969).

³R. Chuckrow and H. H. Stroke, *J. Opt. Soc. Am.* **61**, 218 (1971).

⁴C. M. Lederer, J. M. Hollander, and I. Perlman, *Table of Isotopes* (Wiley, New York, 1967), 6th ed.

⁵This number is an average value calculated from the measured spins, moments, and splitting factors for all mercury isotopes.

⁶A. R. Bodmer, *Nucl. Phys.* **9**, 371 (1959).

⁷A. R. Bodmer, Proc. Phys. Soc. (London) **A67**, 622 (1954).

⁸A. S. Meligy, Nucl. Phys. **16**, 99 (1960).

⁹S. Mrozowski, Phys. Rev. **57**, 207 (1940).

¹⁰H. Kopfermann, *Nuclear Moments* (Academic, New York, 1958).

¹¹G. Breit, Rev. Mod. Phys. **30**, 507 (1958).

¹²P. Brix and H. Kopferman, Rev. Mod. Phys. **30**, 517 (1958).

¹³D. A. Shirley, Rev. Mod. Phys. **36**, 339 (1964).

¹⁴B. Hahn, D. G. Ravenhall, and R. Hofstadter, Phys. Rev. **101**, 1131 (1956).

¹⁵R. C. Barrett, Nucl. Phys. **88**, 128 (1966).

PHYSICAL REVIEW C

VOLUME 5, NUMBER 4

APRIL 1972

Emission of Alpha Particles in the Fission of ²³⁸U by 16- and 42-MeV Protons*

M. Rajagopalan† and T. D. Thomas‡

Department of Chemistry, Princeton University, Princeton, New Jersey 08540

(Received 24 January 1972)

The rate of emission of α particles in coincidence with fission has been measured for ²³⁸U bombarded with protons of energy 16 and 42 MeV. There is a significant increase in the number of α particles per fission over this range. Part of this increase is due to contributions from the $(p, \alpha f)$ reaction. After corrections are made for this process, however, there remains an increase of about 20% in the probability for the $(p, f\alpha)$ reaction between the low- and high-energy measurements. These results together with those of others can be summarized by the formula $Y_\alpha = 1.82 \pm 0.13 + (0.019 \pm 0.006)E^*$, where Y_α is the number of long-range α particles per thousand fissions and E^* is the excitation energy. This dependence on energy can be understood by assuming that the α particles arise from the fragments that are most deformed at the scission point. Although the average deformation at scission remains approximately constant with excitation energy, the spread in the distribution of deformations and, hence, the number of configurations with high deformation, may increase with excitation energy. The angular correlation between fission fragments and α particles near 90° is independent of the excitation energy. At 180°, however, there is a marked increase in the number of coincidences as the excitation energy is increased.

INTRODUCTION

Although the probability of α -particle emission in fission has been measured for different fissioning systems and for different excitation energies over the years, there have been considerable discrepancies among the various values reported. It has been definitely established that the probability of α -particle emission in thermal-neutron-induced fission is less than the probability in spontaneous fission of the same fissioning species.¹ For excitation energies above the neutron separation energy there have been conflicting results: Perfilov, Solov'eva, and Filov² reported that the α -particle-emission rate in the 14-MeV neutron-induced fission of ²³⁵U was less than that in the thermal-neutron fission of the same nucleus. Coleman, Fairhall, and Halpern³ reported an increase in the probability of α -particle emission with increase in excitation energy in the fission of ²³⁸U induced by α particles of energy in the range 29–42 MeV. These observations led to the belief that the probability of α -particle emission at first decreases with an increase in excitation energy up to an excitation energy of 20 MeV and then in-

creases with an increase in excitation energy. However, later work led to a modification of this view. Drapchinski, Kovalenko, Petrzhak, and Tyutyugin⁴ found that the results reported by Perfilov, Solov'eva, and Filov were in error and that the probability of α -particle emission remains the same in the fission of ²³⁵U induced by slow neutrons, 2.5- and 14-MeV neutrons. It is now generally agreed that after an initial decrease as the excitation energy is increased from 0 to about 6 MeV, there is no further decrease in the probability of α -particle emission as the excitation energy is increased. However, the question of whether the α -particle emission in fission increases with excitation energy or remains constant has remained unclear. There are still conflicting reports regarding this question. Recent investigations in the Soviet Union show that there is no appreciable increase in the probability of α -particle emission in 14-MeV neutron-induced fission compared to that in reactor neutron-induced fission of ²³⁵U,^{5,6} and ²³²Th.⁶ However, Nagy, Nagy, and Vinnai⁶ reported an increase in the probability of α -particle emission in the fission of ²³⁸U induced by 14-MeV neutrons compared to the

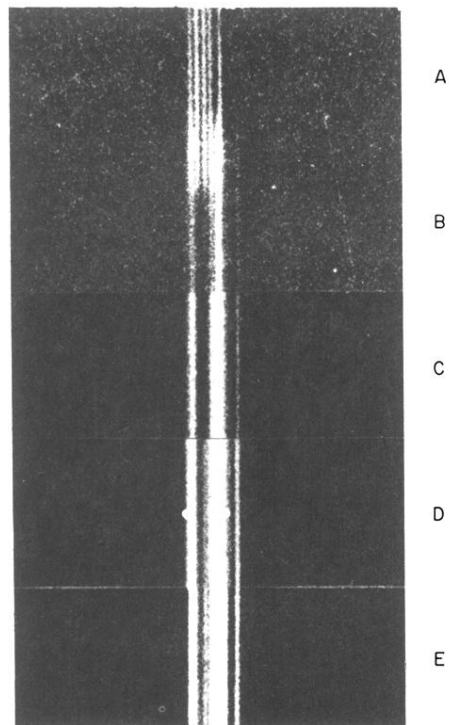


FIG. 1. Spectrograms of the mercury 2537-Å line: A, natural mercury; B, C, D, radioactive mercury about 35 min after beam-off time. The two white dots in D show 199m components; E shows radioactive mercury about 8 h after beam-off time.